Vietnam Journal of Earth Sciences, 43(1), 71-80, https://doi.org/10.15625/0866-7187/15704

Vietnam Academy of Science and Technology
Vietnam Journal of Earth Sciences
http://www.vjs.ac.vn/index.php/jse

Removal of chromium from wastewater using paper waste sludge-derived hyrdrochar modified by NaOH

Lan Huong Nguyen[1], Huu Tap Van[2*], Quang Trung Nguyen[2], Thu Huong Nguyen[2], Thi Bich Lien Nguyen[2], Thi Phuong Thuy Pham[3], Viet The Ho[3], Thai Hoang Le[4], Manh Ha Bui[5], Ordanza Hanna Joy Tilpo[6], Marcaida Gio Serafin Ivan Jimenez[6], Tra Mai Ngo[7]

[1]*Faculty of Environment - Natural Resources and Climate Change, Ho Chi Minh City University of Food Industry (HUFI), Ho Chi Minh City, Vietnam*
[2]*Faculty of Natural Resources and Environment, TNU - University of Sciences (TNUS), Tan Thinh Ward, Thai Nguyen City, Vietnam*
[3]*Faculty of Biological Technology, Ho Chi Minh City University of Food Industry (HUFI), Ho Chi Minh City, Vietnam*
[4]*Department of Environmental Engineering, International University, Vietnam National University, Ho Chi Minh City, Vietnam*
[5]*Department of Environmental Sciences, Saigon University, Ho Chi Minh City, Vietnam*
[6]*Department of Environmental Science and Management, Advanced Education Program - TNU - University Agriculture and Forestry (TUAF), Quyet Thang Ward, Thai Nguyen City, Vietnam*
[7]*Institute of Physic, VAST, Hanoi, Vietnam*

Received 6 August 2020; Received in revised form 10 November 2020; Accepted 15 December 2020

ABSTRACT

In this work, paper waste sludge (PWS) collected from the primary settling tank of the paper wastewater treatment plant was utilized to generate hydrochar as a low-cost adsorbent for Cr(VI) removal from aqueous solution. The characteristics of paper waste sludge hydrochar (PWSH) and the effect of Cr(VI) adsorption conditions onto PWSH, including solution pH (3-9), contact time (5-240 min), initial Cr(VI) concentration (10-80 mg/L) and the adsorbent dose of 1 g/L at room temperature (25±2°C) were investigated. Adsorption isotherm and kinetics were also predicted in this work. The results indicate that the maximum adsorption capacity achieved 11.89 mg/g at 120 min of contact time, pH 3, and initial Cr(VI) concentration of 60 mg/L. The adsorption isotherm was reflected the best by the Langmuir model (R^2 of 0.9968). Whereas, the adsorption kinetic also indicates that the pseudo-second-order model predicted the best for Cr(VI) adsorption process with a R^2 of 0.9469. The mechanism of Cr(VI) adsorption process onto PWSH was chemical sorption through electrostatic interaction and ion exchange.

Keywords: Chromium, hydrochar, adsorption, paper waste sludge, ion exchange.

1. Introduction

Chromium is a harmful element that has been discharged into receiving water bodies from many industrial wastewater sources, consisting of leather tanning, electroplating, metal processing, paint manufacturing, steel fabrication, dyes, chromate preparation, pigments, inks, cement, mining, glass,

*Corresponding author, Email: tapvh@tnus.edu.vn

ceramics, rubber, and fertilizers (Sheth and Soni, 2005). Hexavalent chromium (Cr(VI)) and trivalent chromium (Cr(III)) are the two main existing forms of chromium in the aqueous solution (Ali et al., 2016). In a water environment, Cr(VI) is more mobile and toxic than Cr(III) about 10-100 times (Vu et al., 2019). For humans, Cr(VI) is more harmful due to causing lung disease, cancer, and other health problems (Khushk et al., 2019).

To date, there have been several techniques that are applied to remove Cr(VI) from wastewater such as chemical precipitation, adsorption, electrocoagulation, ion exchange, membrane separation, reduction, and biosorption (Hoang et al., 2019). Among the above-mentioned methods, adsorption is one of the interesting techniques for Cr(VI) removal from the water environment. Recently, hydrochar has been widely studied to remove pollutants from wastewater due to simple production at low temperature and cost, so it can be used as an effective and low-cost adsorbent. For instance, the agricultural wastes derived hydrochar modified by KOH were prepared and used to remove Cr(VI) from an aqueous solution (Khushk et al., 2019). In another study, KOH and H_3PO_4 modified hydrochars derived from hickory and peanut were applied to adsorb methylene blue and lead from aqueous solutions (Fang et al., 2017). Methylene blue (MB) dye solution was also removed by the hydrochar prepared from male oil palm flower (Said et al., 2020). Other hydrochars were also prepared from biomass-Salix as a low-cost sorbent for the removal of Cr(VI) from an aqueous solution (Lei et al., 2018). In 2020, bisphenol A and diuron were also removed by an adsorption process using Argan Nut Shell-derived hydrochar (Zbair et al., 2018).

Annually, there has been a huge amount of paper waste sludge discharged from wastewater treatment systems all over the world. In Vietnam, the amount of paper waste sludge was released approximately 300 kg/day at each factory. This paper waste sludge was usually used as fuel to provide heat for boilers and other manufacturing processes. However, the utilization of this aim was not effective due to its high moisture and energy consumption.

In the present work, a hydrochar derived from paper waste sludge which was discharged from pulp and paper production process collected from primary settling tank was developed as an effective, low-cost, and new adsorbent for Cr(VI) removal from aqueous solution. The utilization of the paper waste sludge to prepare the hydrochar for the adsorption of Cr(VI) can remarkably contribute to both solid waste management and the production of an environmentally friendly material for the treatment of a toxic trace metal. The aim of this study, therefore, was to develop an absorbent from paper waste sludge as a novel hydrochar that was modified by NaOH based on in situ steps for Cr(VI) removal from aqueous solution. The experiments were conducted to evaluate the effects of pH, contact time, and initial Cr(VI) concentration on adsorption of Cr(VI) onto hydrochar. Adsorption isotherm and kinetics of Cr(VI) onto hydrochar were also used to describe the adsorption mechanism of Cr(VI) from aqueous solution.

2. Materials and methods

2.1. Preparation of NaOH modified hydrochar

At the beginning of the hydrochar fabrication process, the paper waste sludge was collected from the primary settling tank

in the wastewater treatment system of Hoang Van Thu Paper Joint Stock Company, Thai Nguyen city, Thai Nguyen province, Vietnam. In the next step, a certain amount of paper waste sludge was dried in an oven at 105°C for 48 h. Subsequently, hydrothermal carbonization of PWS was conducted in a Teflon-lined stainless steel autoclave reactor. The hydrothermal carbonization was performed as follows: firstly, 10 g of above-dried paper waste sludge was mixed with 40 mL of NaOH 0.25 M and put into a Teflon-lined stainless steel autoclave reactor of 300 mL. Later, the autoclave was heated at 200°C for 24 h with a heating rate of 10°C in a furnace. At the end of the process, it was taken out from the furnace and cooled to ambient temperature (Qian et al., 2018). The obtained hydrochar was filtered and washed to discard residues with deionized water until pH of 7.0, then dried at 105°C for 2 h. Finally, the obtained hydrochar was sieved to a size of less than 0.5 mm and stored in the bag for the next usage.

Characteristics of PWSH were evaluated via measurements of BET using Brunauer-Emmett-Teller (BET- BET, Builder, SSA-4300), scanning electron microscope (SEM) images of energy-dispersive X-ray spectroscopy (Hitachi S-4800), FTIR of Fourier transform infrared spectroscopy (FT/IR-6300) in the 4000-500 cm^{-1} ranges. The pH at the point of zero charges (pH_{PZC}) was determined by the shift method (Zhao et al., 2016).

2.2. Batch adsorption experiments

In this work, a wide range of parameters of the adsorption process of Cr(VI) onto PWSH that consisted of pH (2-9), contact time (5-240 min), and initial Cr(VI) concentration (10-80 mg/L) were examined to determine the adsorption capacity, adsorption isotherm and kinetics of Cr(VI) onto PWSH. All batch adsorption experiments were conducted in Erlenmeyer flasks of 50 mL containing 25 mL of solution with initial Cr(VI) concentration, pH values, and contact time as above mentioned and 1 g/L of PWSH. In detail, towards the experiments for the effect of the pH value, the contact time, and initial Cr(VI) concentration were kept constant at 60 min and 30 mg/L, respectively. Adsorption time was varied from 5 to 240 min to evaluate the effects of contact time on Cr(VI) adsorption onto PWSH with the suitable pH value found in the previous experiment, PWSH dosage of 1 g/L and 30 mg/L of initial Cr(VI). For the experiment about investigation effect of the initial Cr(VI) concentration, the initial Cr(VI) concentration was varied from 10 to 80 mg/L with the suitable pH and contact time found in the previous experiments. The flasks were then shaken at 120 rpm on a shaker (PH-4A, China) at the room temperature of 25±2°C. At the end of each experiment, the samples were filtered using a ø45 μm filter membrane to separate solid from the liquid.

The obtained liquid solution then was used to determine left Cr concentration using Inductively Coupled Plasma - Optical Emission Spectrometry (ICP-OES, Model: ULTIMA EXPERT, Horiba, France). Cr(VI) standard solution was used to set up the Cr(VI) standard curve by the software of ICP-OES equipment. In the next step, the samples containing Cr(VI) before and after the adsorption process were automatically pumped into a plasma incineration chamber in which oxidation reaction occurred and ICP-OES would automatically analyze and computed Cr concentration in samples based on the standard curve.

The Cr(VI) amount adsorbed onto PWSH at any time t (q_t, mg/g) and equilibrium (q_e, mg/g) were determined by the equations as follows:

$$q_e = \frac{(C_o - C_e)V}{W} \quad (1)$$

$$q_t = \frac{(C_o - C_t)V}{W} \quad (2)$$

where, C_0, C_t and C_e(mg/L), respectively, are concentrations of Cr(VI) at beginning time, any time *t*, and equilibrium. V(L) is the volume of solution (L) and W(g) is the dry amount of PWSH.

2.3. Adsorption isotherm and kinetic

The Langmuir, Freundlich and Sips models were used to analyze the adsorption isotherm of Cr(VI) onto PWSH. The Langmuir and Freundlich models presume that the adsorption process is monolayer adsorption (Langmuir, 1918), multilayer adsorption (Zhang et al., 2018), respectively and the Sips model is a combination of the Freundlich and Langmuir models (Zhou et al., 2018). The following Equations of (3), (4) and (5) were applied to describe the Langmuir, Freundlich and Sips models, respectively:

$$q_e = \frac{q_m K_L C_e}{1 + K_L C_e} \quad (3)$$

$$q_e = K_F C_e^{\frac{1}{n}} \quad (4)$$

$$q_e = \frac{q_m (bC_e)^{\frac{1}{n}}}{1 + (bC_e)^{\frac{1}{n}}} \quad (5)$$

where, q_e (mg/g) and q_m (mg/g) and C_e (mg/L) are the adsorption capacity at equilibrium, the maximum saturated adsorption capacity, and the adsorbate concentration at equilibrium; K_L (L/mg) is the Langmuir constant related to the energy of the adsorption, and K_F (mg/g) is the Freundlich constant.

Whereas, equations of (6) and (7) were used to describe the pseudo-first-order and pseudo-second-order models, respectively. These models were used to analyze adsorption kinetics.

$$q_t = q_e(1 - e^{-k_1 t}) \quad (6)$$

$$q_t = \frac{q_e^2 k_2 t}{1 + q_e k_2 t} \quad (7)$$

where, q_e (mg/g), q_t (mg/g), k_1 (min^{-1}), k_2 (g/mg.min), α (mg/g min) and β (g/mg) are the adsorption capacity at equilibrium and at time t, the first-order rate constant, the second-order rate constant, the initial adsorption rate and the adsorption constant, respectively.

2.4. Data analysis

All experiments were performed in duplicate. All data statistics, including means, standard deviations, relative standard deviations and regressions (linear) were computed with tools in MS excel software and origin 9.0 software. The highest acceptable deviation was 5%. The error bars indicating the standard deviation were shown in all figures wherever possible.

3. Result and discussion

3.1. Characteristic of paper waste sludge hydrochar

The BET surface area (S_{BET}) and total pore volume of PWSH were smaller than 2 m^2/g and 0.001 cm^3/g, respectively. Fig. 1 shows the characteristics of paper waste sludge hydrochar after treated by NaOH. The results of SEM analyses indicate the surface morphology of PWSH (Fig. 1a). From Fig. 1a, as can be seen, the paper waste sludge hydrochar possessed a porous and rough structure. The dominant functional groups on the PWSH's surface were identified by the FTIR spectra (Fig. 1b). The data from Fig. 1b shows there was a broad peak at around 3699 and 2914 cm^{-1} assigned to the vibration of O-H stretching and C-H groups, respectively. The peak at 2523 cm^{-1} contributed to the O-H group. Whereas, these peaks at 1794 cm^{-1}, 1159 cm^{-1}, 916 cm^{-1}, 873 cm^{-1}, and 661 cm^{-1} indicate the presence of the carbonate group's C-O stretching vibration (Nan et al., 2008; Tizo et al., 2018).

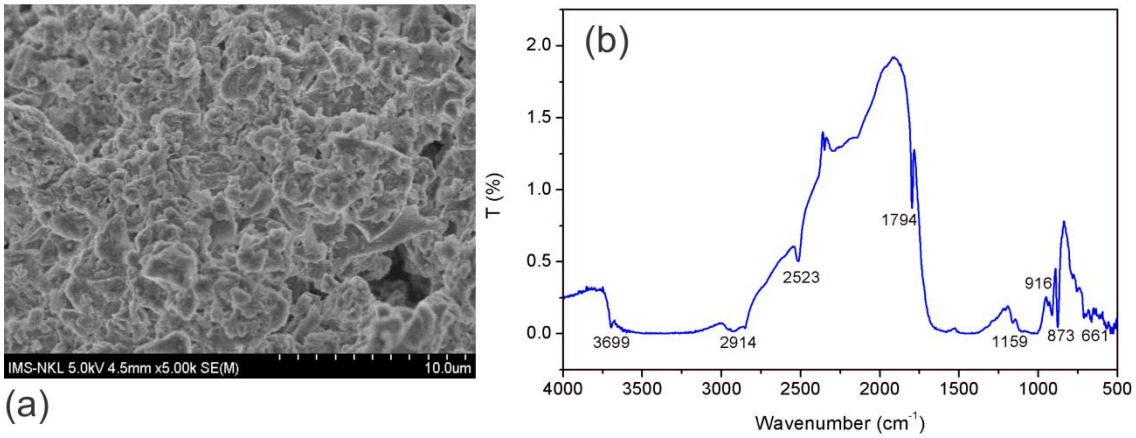

Figure 1. Characteristics of PWSH: (a) SEM image, (b) FTIR spectra

3.2. Effect of pH

The pH value of an aqueous solution containing Cr(VI) is one of the major factors affecting on adsorption process of Cr(VI) onto PWSH. In this study, a wide range of solution pH values from 2 to 9 were investigated for Cr(VI) adsorption process at initial Cr(VI) concentration of 30 mg/L, PWSH dosage of 1 g/L, and contact time of 60 min at room temperature (25±2°C). The adsorption capacity and removal efficiency of Cr(VI) are presented in Fig. 2. As can be seen from Fig.2, the adsorption capacity of Cr(VI) onto PWSH decreased with increased solution pH values from 3 to 9. In detail, at pH 3, the maximum adsorption capacity and removal efficiency of Cr(VI) achieved 5.96 mg/g and 39.75%, respectively. This can be explained as due to the co-existence of various forms of Cr(VI) in the solution. With the solution pH of 3, the dominant form of Cr(VI) was $HCrO_4^-$ (Akram et al., 2017) and CrO_4^{2-} at higher pH values (Huang et al., 2015). Additionally, the surface of hydrochar is positively charged at low pH and negatively charged at high pH (Ullah et al., 2013). Thereby, Cr(VI) adsorption capacity and efficiency were higher at low pH value due to protonation and electrostatic attraction between $HCrO_4^-$ and acidic functional groups of PWSH. There was an increase in the number of protons on the PWSH's surface at lower pH leading to the enhancement of the attraction between $HCrO_4^-$ and functional groups on PWSH's surface. However, with the increase in the pH value, the adsorbent's surface became negatively charge resulting in the generation of repulsive forces between Cr(VI) ions and adsorbent (Akram et al., 2017). Therefore, the adsorption capacity of Cr(VI) onto PWSH decreased with the increase in solution pH. In the present work, a suitable solution pH for Cr(VI) adsorption onto PWSH was 3. A similar trend was reported by previous works such as the reports of Cr(VI) adsorption onto bio-composite of mango (Mangifera indica) (Akram et al., 2017), magnetic biochar derived from Melia azedarach wood (Zhang et al., 2018), and magnetic modified-corncob biochar (Hoang et al., 2019).

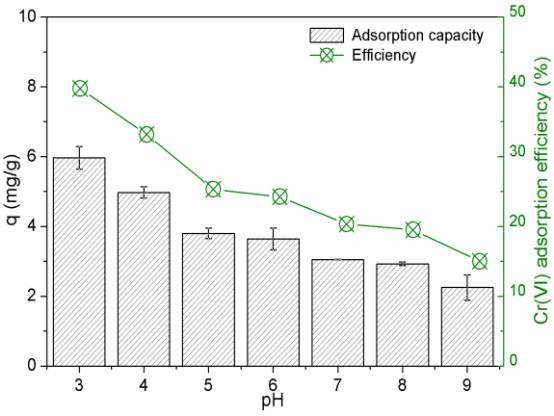

Figure 2. Effect of pH on Cr(VI) adsorption onto PWSH. Experimental conditions: Cr(VI): 30 mg/L, adsorbent dose: 1 g/L, contact time: 60 min

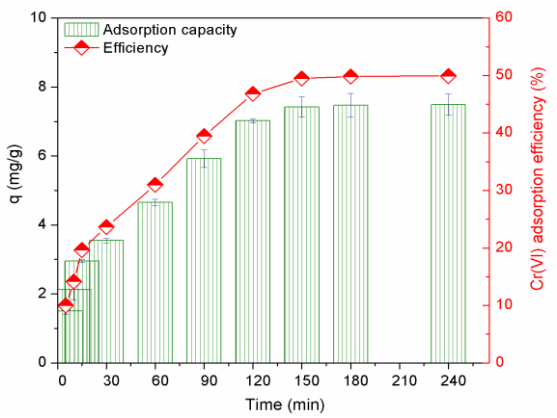

Figure 3. Effect of contact time on Cr(VI) adsorption onto PWSH. Experimental conditions: Cr(VI): 30 mg/L, adsorbent dose: 1 g/L, pH: 3

3.3. Effect of contact time

The effect of contact time on Cr(VI) adsorption was investigated up to 240 min at pH 3, 30 mg/L of initial Cr(VI) concentration, and PWSH dosage of 1 g/L. The results of Cr(VI) adsorption capacity and efficiency are demonstrated in Fig. 3. Obviously, there was a rapid increase in adsorption capacity and removal efficiency of Cr(VI) by PWSH when contact time went up from 5 min to 120 min. By further increasing up to 150 min, adsorption capacity and removal efficiency of Cr(VI) increased slightly and remained almost constant with higher contact time. This trend can be explained that at the initial stage of the adsorption process, active sites on the hydrochar's surface were freely available to bind Cr(VI) leading to quick adsorption. However, there was a decrease in active sites corresponding to slow adsorption with further increasing of contact time (Gupta and Balomajumder 2015). A similar trend was reported by previous works in Cr(VI) adsorption from aqueous solution by feedstock hydrochar (Iyer et al., 2019) and freshwater snail shell (Vu et al., 2019).

3.4. Effect of initial Cr(VI) concentration

Initial Cr(VI) concentration varied from 10 to 80 mg/L at pH 3, adsorbent dose of 1 g/L, 120 min of contact time at room temperature to evaluate the adsorption capacity and removal efficiency of Cr(VI) onto PWSH. The obtained results are illustrated in Fig. 4. What stands out from the data in Fig. 4 is that the adsorption capacity increased linearly from 3.64 mg/g to 11.89 mg/g corresponding to an increase in initial Cr(VI) concentration from 10 mg/L to 60 mg/L and remained nearly constant with further higher concentration. This trend can be explained that although there were constantly available active sites on PWSH's surface for all experimental conditions there was an increase in the amount of Cr(VI) ions from solution leading to the increase in the ratio of the amount of Cr(VI) ions and the available adsorption sites, thus, more Cr(VI) ions were adsorbed on PWSH (Huang et al., 2015). On the contrary, the removal efficiency of Cr(VI) decreased from 72.70% to 31.00% with an increase in initial Cr(VI) concentration from 10 mg/L to 80 mg/L due to the same amount of PWSH for each adsorption condition but initial Cr(VI) concentration increased.

Therefore, most Cr(VI) ions were attracted by PWSH's surface with low Cr(VI) concentration in solution but there were still some Cr(VI) ions that were not adsorbed with increasing Cr(VI) concentration in solution leading to a decrease in the removal efficiency. Similar trends were recorded in the adsorption of heavy metals onto natural limestone (Sdiri et al., 2012), Cr(VI) removal by magnetite snail shell (Hoang et al., 2020), and wheat shell (Saha et al., 2012).

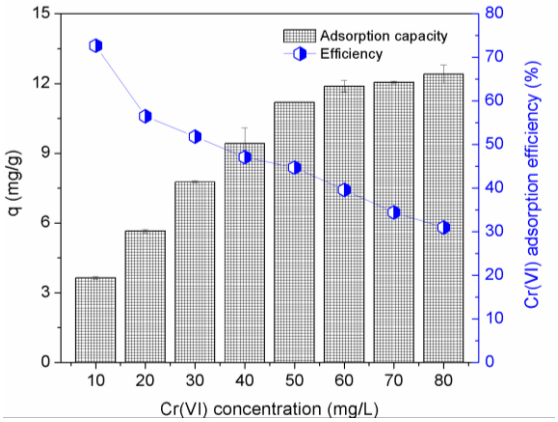

Figure 4. Effect of initial Cr(VI) concentration on Cr(VI) adsorption onto PWSM. Experimental conditions: pH: 3, contact time: 120 min, adsorbent dose: 1g/L

3.5. Adsorption isotherm

In order to analyze the adsorption isotherm of Cr(VI) onto PWSH, several models, including Langmuir, Freundlich, and Sips, were used to fit experimental data. The calculated data from fitting three isotherm models are presented in Table 1 and Fig. 5. What stands out from the data in both Table 1 and Fig. 5 is that all three adsorption isotherm models were fitted well with experimental data with a high correlation coefficient (R^2) of 0.9968, 0.9969 and 0.9896 for Langmuir, Sips and Freundlich models, respectively. However, the Langmuir model described the best adsorption of Cr(VI) onto PWSH with the calculated q_m of 16.54 mg/g compared to q_{mexp} (12.40 mg/g). This illustrated that the monolayer adsorption or a fixed number of active sites on PWSH's surface and Cr(VI) ions were the main adsorption mechanisms (Shang et al., 2016). The adsorption of Cr(VI) also was favorable based on Langmuir, Freundlich and Sips models due to the low R_L value of Langmuir model of 0.0202 < 1, K_f value > 1, the 1/n and b values < 1 (Hoang et al., 2020). Similar results were reported by previous studies of Cr(VI) adsorption by magnetic multi-wall carbon nanotubes (Huang et al., 2015) and agricultural waste biomass (Garg et al., 2007).

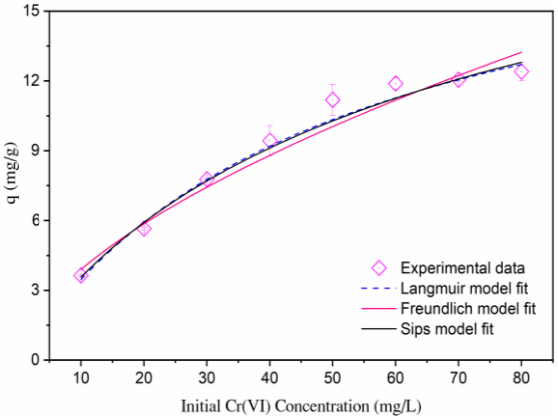

Figure 5. Adsorption isotherm of Cr(VI) onto PWSH

Table 1. Adsorption isotherm parameters of Cr(VI) onto PWSH

Langmuir model			Freundlich model			Sips model				q_{mexp} (mg/g)
q_m (mg/g)	K_L	R^2	K_F	1/n	R^2	q_m (mg/g)	1/n	b	R^2	11.89
16.54	0.0202	0.9968	1.0065	0.587	0.9896	20.64	0.911	0.0218	0.9969	

3.6. Adsorption kinetic

Adsorption kinetics of Cr(VI) onto PWSH are presented in Fig. 6 and Table 2. The calculated results of correlation coefficient values (R2) from pseudo-first-order and pseudo-second-order models, respectively, were 0.9125 and 0.9469. According to R2 values, the adsorption dynamic of Cr(VI) fit fairly well to both models. Nevertheless, R^2 of the pseudo-second order model was slightly higher in comparison with the pseudo-first order model. Besides, the calculated q_e value of pseudo-first order and pseudo-second order models reached 6.98 mg/g and 7.67 mg/g, respectively. The calculated results illustrate that both kinetic models were suitable to describe Cr(VI) adsorption process by PWSH. It also suggested that the Cr(VI) adsorption process by PWSH was the chemical adsorption through ion exchange and electrostatic interaction (Kera et al., 2017). The similar calculated results were reported by other works, such as a study on using activated charcoal (Sika et al., 2010) and polypyrrole coated palygorskite (Yao et al., 2012) for Cr(VI) removal from aqueous solution.

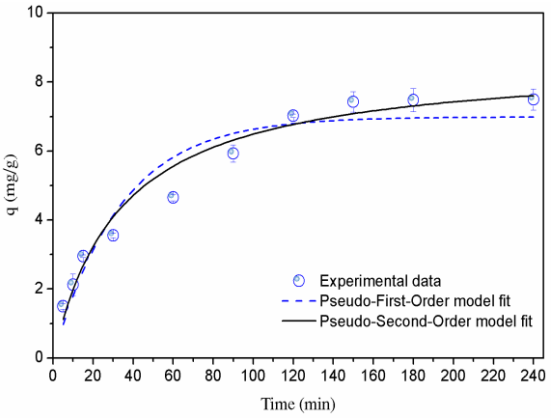

Figure 6. Adsorption kinetic models of Cr(VI) onto PWSH

Table 2. Adsorption kinetic parameters of Cr(VI) onto PWSH

Pseudo-first order			Pseudo-second order			$q_{e,exp}$ (mg/g)
$q_{m,cal}$ (mg/g)	K_1 (1/min)	R^2	$q_{m,cal}$ (mg/g)	K_2 (g/mg×min)	R^2	
6.98	0.02983	0.9125	7.67	0.00343	0.9469	7.43

4. Conclusions

The paper waste sludge hydrochar (PWSH) was a good adsorbent for Cr(VI) adsorption from aqueous solution. This study showed the potential of reuse of solid waste (paper waste sludge) as a low-cost adsorbent for effective Cr(VI) removal from aqueous solution. The adsorption results of Cr(VI) onto PWSH at various experimental conditions indicate that suitable conditions of Cr(VI) removal occurred at pH 3.0, the contact time of 120 min, initial Cr(VI) concentration of 60 mg/L, and PWSH dose of 1.0 g/L at room temperature. The maximum adsorption capacity of Cr(VI) from aqueous solution by PWSH was 11.89 mg/g. The Cr(VI) adsorption capacity calculated by the Langmuir model was 16.54 mg/g. Both pseudo-first-order and pseudo-second-order models fit well to experimental data of Cr(VI) adsorption. Additionally, the characteristics of PWSH were very useful for Cr(VI) removal from aqueous solution. However, this study only was batch adsorption and was conducted at a lab-scale. Thus, it is essential to further investigate several criteria, including the durability, desorption, and regeneration, applicability, cost of this hydrochar other studies to assess potentially reaching QCVN: 40-2011/BTNMT and application in practice.

Acknowledgements

This research is funded by Vietnam National Foundation for Science and

Technology Development (NAFOSTED) under grant number 105.08-2019.07.

References

Akram M., Bhatti H. N., Iqbal M., Noreen S., Sadaf S., 2017. Biocomposite efficiency for Cr(VI) adsorption: Kinetic, equilibrium and thermodynamics studies. J. Envi. Chem. Engin., 5(1), 400-411.
https://doi.org/10.1016/j.jece.2016.12.002.

Ali A., Saeed K., Mabood F., 2016. Removal of chromium (VI) from aqueous medium using chemically modified banana peels as efficient low-cost adsorbent. Alexandria Engin. J., 55(3), 2933-2942. https://doi.org/10.1016/j.aej.2016.05.011.

Fang J., Gao B., Mosa A., Zhan L., 2017. Chemical activation of hickory and peanut hull hydrochars for removal of lead and methylene blue from aqueous solutions. Chem. Specia. Bioavai., 29(1), 197-204. https://doi.org/10.1080/09542299.2017.1403294.

Garg U.K., Kaur M.P., Garg V.K., Sud D., 2007. Removal of hexavalent chromium from aqueous solution by agricultural waste biomass. J. Haza. Mater., 140(1-2), 60-68.
https://doi.org/10.1016/j.jhazmat.2006.06.056.

Gupta A., Balomajumder C., 2015. Simultaneous adsorption of Cr(VI) and phenol onto tea waste biomass from binary mixture: Multicomponent adsorption, thermodynamic and kinetic study. J. Envi. Chem. Engin., 3(2), 785-796. https://doi.org/10.1016/j.jece.2015.03.003.

Hoang L.P., Nguyen T.M. P., Van H.T., Hoang T.K.D., Vu X.H., Nguyen T.V., Ca N.X., 2020. Cr(VI) Removal from Aqueous Solution Using a Magnetite Snail Shell. Water, Air. Soil Poll., 231(1), 1-13. https://doi.org/10.1007/s11270-020-4406-4.

Hoang L.P., Van H.T., Nguyen L.H., Mac D.H., Vu T.T., Ha L.T., Nguyen X.C., 2019. Removal of Cr(vi) from aqueous solution using magnetic modified biochar derived from raw corncob. New J. Chem., 43(47), 18663-18672. https://doi.org/10.1039/c9nj02661d.

Huang Z. Nan, Wang X. Ling, Yang D. Suo., 2015. Adsorption of Cr(VI) in wastewater using magnetic multi-wall carbon nanotubes. Wat. Sci. Engin., 8(3), 226-232. https://doi.org/10.1016/j.wse.2015.01.009.

Iyer A., Pensini E., Singh A., 2019. Removal of hexavalent chromium from water using hydrochar obtained with different types of feedstock. Canad. J. Civil Engin, https://doi.org/10.1139/cjce-2019-0215.

Kera N.H., Bhaumik M., Pillay K., Sinha Ray S., Maity A., 2017. Selective removal of toxic Cr(VI) from aqueous solution by adsorption combined with reduction at a magnetic nanocomposite surface. J. Colloid. Interf. Sci., 503, 214-228 https://doi.org/10.1016/j.jcis.2017.05.018.

Khushk S., Zhang L., Pirzada A.M., Irfan M., Li A., 2019. Cr(VI) heavy metal adsorption from aqueous solution by KOH treated hydrochar derived from agricultural wastes. AIP Conf. Proceed., https://doi.org/10.1063/1.5115362.

Langmuir I., 1918. The adsorption of gases on plane surfaces of glass, mica and platinum. J. Ameri. Chem. Soci., 40(9), 1361-1403. https://doi.org/10.1021/ja02242a004.

Lei Y., Su H., Tian F., 2018. A Novel Nitrogen Enriched Hydrochar Adsorbents Derived from Salix Biomass for Cr (VI) Adsorption. Scientific Reports, 8(1), 1-9. https://doi.org/10.1038/s41598-018-21238-8.

Nan Z., Shi Z., Yan B., Guo R., Hou W., 2008. A novel morphology of aragonite and an abnormal polymorph transformation from calcite to aragonite with PAM and CTAB as additives. J. Colloid. Interf. Sci., 317(1), 77-82.
https://doi.org/https://doi.org/10.1016/j.jcis.2007.09.015.

Qian W.C., Luo X.P., Wang X., Guo M., Li B., 2018. Removal of methylene blue from aqueous solution by modified bamboo hydrochar. Ecotoxic. Envi. Saf., 157, 300-306. https://doi.org/10.1016/j.ecoenv.2018.03.088.

Saha P. Das, Dey A., Marik P., 2012. Batch removal of chromium (VI) from aqueous solutions using wheat shell as adsorbent: Process optimization using response surface methodology. Desali. Wat. Treat., 39(1-3), 95-102. https://doi.org/10.1080/19443994.2012.669164.

Said A., Tekasakul S., Phoungthong K., 2020. Investigation of hydrochar derived from male oil palm flower: Characteristics and application for dye removal. Polish J. Envir. Stud., 29(1), 807-816. https://doi.org/10.15244/pjoes/103355.

Sdiri A., Higashi T., Jamoussi F., Bouaziz S., 2012. Effects of impurities on the removal of heavy metals by natural limestones in

aqueous systems. J. Envir.l Manag., 93(1), 245-253. https://doi.org/https://doi.org/10.1016/j.jenvman.2011.08.002.

Shang J., Pi J., Zong M., Wang Y., Li W., Liao Q., 2016. Chromium removal using magnetic biochar derived from herb-residue. J. Taiwan Inst. Chem. Eng., 68, 289-294. https://doi.org/10.1016/j.jtice.2016.09.012.

Sheth K.N., Soni V.M., 2005. Comparative study of removal of Cr(VI) with PAC, GAC and adsorbent prepared from tobacco roots. J. Envir. Sci. Engin., 47(3), 218-221.

Sika M.S., Liu F., Chen H., 2010. Optimization of key parameters for chromium (VI) removal from aqueous solutions using activated charcoal. J. Soil Sci. Envir. Manag., 1(3), 55-62.

Tizo M.S., et al., 2018. Efficiency of calcium carbonate from eggshells as an adsorbent for cadmium removal in aqueous solution. Susta. Envi. Res., 28(6), 326-332.

https://doi.org/https://doi.org/10.1016/j.serj.2018.09.002

Ullah I., Nadeem R., Manzoor Q., 2013. Biosorption of chromium onto native and immobilized sugarcanebagasse waste biomass. Ecolo. Engin., 60, 99-107.

https://doi.org/10.1016/j.ecoleng.2013.07.028.

Vu X.H., Nguyen L.H., Van H.T., Nguyen D.V., Nguyen T.H., Nguyen Q.T., Ha L.T., 2019. Adsorption of chromium(VI) onto freshwater snail shell-derived biosorbent from aqueous solutions: Equilibrium, kinetics, and thermodynamics. J. Chem., (Iii). https://doi.org/10.1155/2019/3038103.

Yao C., et al., 2012. Polypyrrole/palygorskite nanocomposite: A new chromate collector. Appl. Clay Sci., 67-68, 32-35.

https://doi.org/https://doi.org/10.1016/j.clay.2012.07.007

Zbair M., et al., 2018. Hydrothermal Carbonization of Argan Nut Shell: Functional Mesoporous Carbon with Excellent Performance in the Adsorption of Bisphenol A and Diuron. Wast. Bioma. Valor., 11(4), 1565-1584. https://doi.org/10.1007/s12649-018-00554-0.

Zhang Xiaonuo, Lin X., He Y., Chen Y., Zhou J., Luo X., 2018. Adsorption of phosphorus from slaughterhouse wastewater by carboxymethyl konjac glucomannan loaded with lanthanum. Inter. J. Biolog. Macromol., 119, 105-115. https://doi.org/https://doi.org/10.1016/j.ijbiomac.2018.07.140.

Zhang Xin, et al., 2018. Removal and recovery of Cr(VI) from wastewater by maghemite nanoparticles. Water Res, 256(18), 1-10. https://doi.org/https://doi.org/10.1016/j.watres.2005.05.051.

Zhao B., Zhang J., Yan W., Kang X., Cheng C., 2016. Removal of cadmium from aqueous solution using waste shells of golden apple snail. Desali, Wat. Treat., 3994, 23987-24003. https://doi.org/10.1080/19443994.2016.1140078.

Zhou X., Liu Y., Zhou J., Guo J., Ren J., Zhou F., 2018. Efficient removal of lead from aqueous solution by urea-functionalized magnetic biochar: Preparation, characterization and mechanism study. J. Taiwan Inst. Chem. Engin., 91, 457-467.

https://doi.org/https://doi.org/10.1016/j.jtice.2018.04.018.